Vol 14 No 12, December 2005
1009-1963/2005/14(12)/2539-07

Chinese Physics

© 2005 Chin. Phys. Soc.
and IOP Publishing Ltd

The carbon impurity particle transport in ohmic discharges on the HT-7 tokamak*

Zhou Qian(周 倩)†, Wan Bao-Nian(万宝年),
Wu Zhen-Wei(吴振伟), and Huang Juan(黄 娟)

Institute of Plasma Physics, Chinese Academy of Sciences Hefei 230031, China

(Received 18 March 2005; revised manuscript received 8 August 2005)

The line-integrated optical measurement of impurity radiation profiles for the study of light impurity transport is performed in the HT-7 tokamak. The carbon impurity line emissivity is obtained by Abel inversion. The radial transport behaviours of carbon impurities at different central line averaged electron densities $\overline{n_e}$ are investigated in ohmic discharges. The diffusion coefficient $D_k(r)$, the convection velocity $W_k(r)$ and the total flux of the impurity ions Γ_k decrease with the increase of $\overline{n_e}$, which shows a reduction in the impurity particle transport at higher electron densities.

Keywords: tokamak, impurity particle transport, diffusion coefficient, convection velocity
PACC: 5225F, 5225V, 5255P

1. Introduction

Impurities play an important role in determining plasma behaviours in tokamaks, and they are responsible for large radiation losses. Plasma resistivity usually is several times higher than that of pure plasma. Impurity particle concentration and their transport, on the other hand, affect the plasma particle and energy balance, and, in some cases, even cause MHD instabilities and disruption.[1] The fully understanding of impurity transport behaviour, in other words, the finding of a method of controlling the impurities in the plasma, is important in the thermonuclear fusion research and the achievement of controlled fusion power. The spectroscopic study of impurity radiation is an important and effective approach to plasma impurity, it can help further understand impurity behaviours in tokamaks.[2]

The effects of neutral particle influx and their ionization on boundary plasmas have been investigated at different central line averaged electron densities by using reciprocating Langmuir probes on the HT-7 tokamak.[3] The boundary electron density gradient and the pressure gradient both become large with the increase of the electron density. The particle and energy confinements are better at higher electron densities, which can be indicated by the decrease in turbulent particle and heat flux. The particle confinement time $\tau_{\rm p}$ estimated from both H_α/D_α emission and electron density $n_{\rm e}$, also increases with the increase of the electron density. The particle perpendicular diffusion coefficient $D_{\rm Turb}$ estimated from the measured turbulent particle flux on the assumption that both the poloidal symmetry is present and the turbulent particle flux is dominant, $D_{\rm SOL}$[4,5] obtained from a simple scrape-off layer (SOL) model, and the Bohm diffusion coefficient $D_{\rm Bohm}$, all decrease with the increase of the electron density. This implies an improvement on particle confinement and reduction in particle transport. It is already concluded that the transport of the particles reduces at higher electron densities, so this paper deals with the impurity particle transport behaviours at different central line averaged electron densities.

The brightness (line integrated) profiles of impurity line emissions have been obtained with an ultraviolet and visible optical measurement system in the HT-7 tokamak, so the emissivity can be obtained by Abel inversion. An impurity transport code,[6] on the assumption that a cylindrical symmetry is present, can be used to derive the diffusion coefficient $D_k(r)$

*Project supported by the National Natural Science Foundation of China (Grant No 10235010).
†E-mail: zhouqian@ipp.ac.cn

and the convection velocity $W_k(r)$ through simulating the experimental results of the emissivity of line emission from ionized light impurities $\varepsilon_k(r)$. Impurity ion densities at various ionization states $n_k(r)/n_0(r_p)$ can be derived by using this code. Because the boron film can suppress the oxygen effectively after boronization ($C_2B_{10}H_{12}$), the carbon from the graphite limiter and boron film is the dominant impurity in the HT-7 tokamak.[7] Therefore, the transport behaviours of carbon impurity are studied in this paper. The different radial transport behaviours of carbon impurities at different central line averaged electron densities in ohmic discharges are investigated in the HT-7 tokamak.

2. HT-7 tokamak

HT-7 is a medium sized super-conducting tokamak with a stainless steel liner and a graphite circular poloidal limiter. Its major radius is 1.22m, and minor radius is 0.27m. The experiments are conducted in deuterium target plasma with a toroidal magnetic field B_ϕ=1–2.5T, plasma current I_P=100–250kA, central line averaged electron density $\overline{n_e}$=0.8–6$\times$ 10^{19}m^{-3}.

Several optical systems are constructed for the measurement of the light impurity radiation profiles in the HT-7 tokamak. The system with a rotating hexahedral mirror for space-time resolved measurements in the ultraviolet and visible spectroscopic ranges can provide the brightness profiles of the light impurity line emission, and it is calibrated absolutely with a standard tungsten lamp. The plasma is scanned in the vertical direction, and two different emission lines of light impurities can be observed in one discharge simultaneously. A center monitoring system (HN) based on both a photodiode detector and a He-Ne laser is used to obtain the information on spatial position during scan. The rising wing of the HN signal pulse corresponds to the center of plasma.

The system of visible multi-channel bremsstrahlung measurement based on interference filters is constructed,[8] and it is calibrated absolutely with a standard tungsten lamp. This system is used to measure the profile of the effective ion charge $Z_{\rm eff}(r)$.

3. Impurity transport model

A 1D impurity transport code[6] is used to determine the impurity ion density profiles of various ionized states and impurity transport coefficient profiles. This code, on the assumption that a cylindrical symmetry is present, takes into account the processes of ionization and recombination. The radial density distributions of the ionized impurities are given by the following set of coupled differential equations:

$$\frac{\partial n_k}{\partial t} + \frac{1}{r}\frac{\partial}{\partial r}(r\Gamma_k) - n_e[(1-\delta_{k,1})\alpha_k n_{k-1} - (\alpha_{k+1}+\beta_k)n_k + \beta_{k+1}n_{k+1}] = \delta_{k,1}n_e\alpha_1 n_0, \quad k = 1,2,...,N, \tag{1}$$

where n_k is the impurity ion density in the kth ionized state, α_k is the ionization rate and given by formula of Lotz.[9] β_k is the total recombination rate (the radiative recombination rate β_k^r[10] and the dielectronic recombination rate β_k^d.[11]) N is the total number of ionized states.

For the steady state solution, $\frac{\partial n_k}{\partial t} = 0$. The flux of the impurity ions in the kth ionized state can be expressed as

$$\Gamma_k = -D_k\frac{\partial n_k}{\partial r} + W_k n_k, \tag{2}$$

where $D_k(r)$ is the diffusion coefficient and $W_k(r)$ is the convection velocity. Both neoclassical transport and anomalous transport are considered. The neoclassical transport coefficients consisting of both diffusion coefficient and convection coefficient, depend on the density and temperature profiles of the background ions, to which contributions can also be made by ions of other impurity elements and ions of the same element in different charged states. In most tokamak experiments, however, it appears that anomalous processes either strengthen or completely dominate the neoclassical transport.[12] To cope with these cases, the simulation code introduces anomalous factors γ_D and γ_W into $D_k^{\rm neo}$ and $W_k^{\rm neo}$ respectively. So $D_k = \gamma_D D_k^{\rm neo}$, $W_k = \gamma_W W_k^{\rm neo}$.

It is assumed that neutral impurities from the limiter and walls flow into the plasma at a thermal velocity, and their density decreases rapidly through ionization as the impurities penetrate into the plasma.

4. Simulation

4.1. Brightness and emissivity

The optical systems are used to measure the brightness B (photons$\cdot$s$^{-1}\cdot$m$^{-2}\cdot$sr^{-1}) of impurity line emission along the line of sight. Since the plasma is optically thin for the lines studied, the brightness B is directly related to the emissivity, ε (photons$\cdot$s$^{-1}\cdot$m^{-3}), by

$$B = \frac{1}{4\pi}\int \varepsilon {\rm d}x, \tag{3}$$

where x is the length of the chord along the line of sight. Figure 1 (a) shows a spatial profile of the CV (227.1nm) brightness in an ohmic discharge. The smoothed brightness curve is also shown in Fig.1(a) by bold solid line. Considering the strong asymmetry in the brightness distribution, the emissivity cannot be obtained by the standard Abel inversion. A special Abel inversion technique is used.[13,14] Figure 1(b) shows the result of Abel inversion.

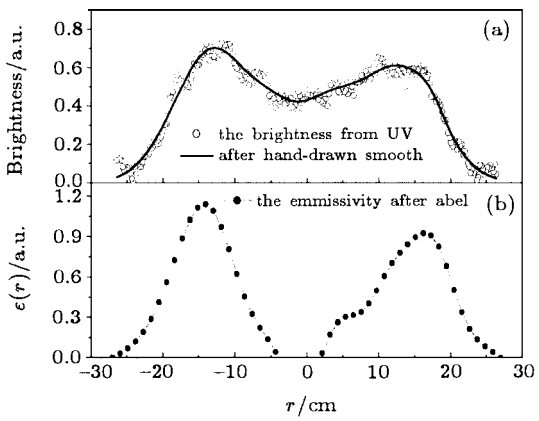


Fig.1. (a) The spatial evolution of the observed CV brightness (circle) and the smoothed brightness curves (solid line). (b) The profile of CV emissivity obtained from the profile in (a) by the special Abel inversion.

4.2. Simulation

The impurity transport code is used to simulate the emissivity of the carbon impurity line emissions, $\varepsilon_k(r)$, by modifying the anomalous diffusion factor γ_D, the anomalous convection factor γ_W and the total concentration of impurities. The diffusion coefficient $D_k(r)$ and the convection velocity $W_k(r)$ of impurity particles are determined by matching the simulation results to the measured profiles of $\varepsilon_k(r)$. Since the peak positions of $\varepsilon_k(r)$ are sensitive to and mainly determined by the transport coefficient of impurities,[15] the extent to which the peak positions of $\varepsilon_k(r)$ obtained from the measurements can accord with those from the code simulation is taken as an indicator of the simulation correctness.

The electron density profile $n_e(r)$, the electron temperature profile $T_e(r)$, the ion temperature profile $T_i(r)$, the H/(H+D) ratio (the ratio of the neutral H in-flux to the total neutral in-flux of H and D), the plasma current I_p and the toroidal magnetic field B_ϕ are the information necessary to the simulation code. The $n_e(r)$ is acquired by a five-channel far-infrared (FIR) hydrogen cyanide (HCN) laser interferometer.[16] The $T_e(r)$ is derived from a compact soft x-ray pulse height analyser (PHA).[17] The Langmuir probe measurements provide the information on the boundary electron density $n_e(r_p)$ and electron temperature $T_e(r_p)$.[3] The $T_i(0)$ is measured by a neutral particle analyser (NPA)[18] and the profile shape of $T_i(r)$ is assumed to be the same as that of $T_e(r)$. The H/(H+D) ratio is derived from the measurements of the optical spectroscopic multi-channel analysis detection (OSMA).[19]

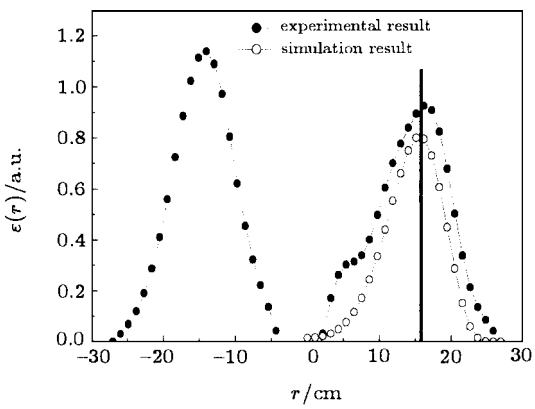


Fig.2. Comparison between experimental results and simulation results of the profile of CV emissivity.

Figure 2 shows a comparison between experimental results and simulation results of the profile of CV line emissivity at 227.1nm. The experimental results are taken from the profiles in Fig.1(b). It is clearly shown that the peak positions of $\varepsilon_{cv}(r)$ of experimental results are in good agreement with those of simulation results, and they are at the same radial position of about 15.7cm.

5. Experimental results

The radial transport behaviours of carbon impurities at different central line averaged electron densities in ohmic discharges are investigated in the HT-7 tokamak.

Shots 54801, 54784 and 54792 of ohmic plasma discharges at different central line averaged electron densities $\overline{n_e}$ are selected for this study. The waveforms for $\overline{n_e}$=1×10^{19} m^{-3} in Shot 54801 (solid), $\overline{n_e}$=1.5×10^{19} m^{-3} in Shot 54784 (dash) and $\overline{n_e}$=2×10^{19} m^{-3} in Shot 54792 (dot) are shown in Fig.3. From the top to the bottom the waveforms are sequentially for plasma current I_p=100kA, loop voltage, central line averaged electron density $\overline{n_e}$, the time-spatial resolved CV brightness at 227.1nm, the HN pulse signal of the center monitoring system, the

H_α/D_α radiation, the bremsstrahlung radiation $I_{\rm br}$, horizontal and vertical positions of plasma. As shown in Figure 3, the plasma current, loop voltage, horizontal and vertical positions of plasma are the same at different $\overline{n_{\rm e}}$. The radiations of H_α/D_α and the bremsstrahlung increase with the increase of $\overline{n_{\rm e}}$. The toroidal magnetic field is $B_\phi \cong 1.85$ T. H/(H+D) ratios in all three discharges are similar within a deviation of about 20%. Because the plasma in the plateau range of discharges: 380–660ms, is in a steady state, the transport behaviours of impurities in this range are considered.

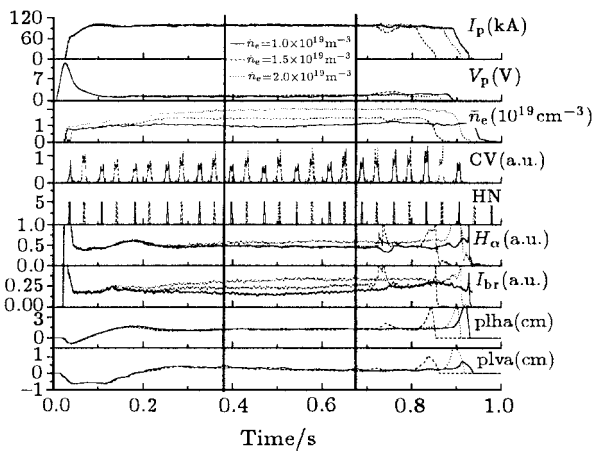


Fig.3. The waveforms of ohmic plasma discharges for $\overline{n_{\rm e}}$=1×10^{19} m^{-3} in Shot 54801 (solid), $\overline{n_{\rm e}}$=1.5×10^{19} m^{-3} in Shot 54784 (dash) and $\overline{n_{\rm e}}$=2×10^{19} m^{-3} in Shot 54792 (dot). From the top to the bottom the waveforms are sequentially for plasma current $I_{\rm p}$, loop voltage $V_{\rm p}$, central line averaged electron density $\overline{n_{\rm e}}$, the time-spatial resolved CV brightness at 227.1nm, the HN pulse signal of the center monitoring system, the H_α/D_α radiation H_α, the bremsstrahlung radiation $I_{\rm br}$, horizontal and vertical positions of plasma.

Through the simulation process described above, the diffusion coefficient $D_k(r)$ and the convection velocity $W_k(r)$ are obtained. Figures 4(a) and (b) show the $D_k(r)$ and $W_k(r)$ for $\overline{n_{\rm e}} = 1\times10^{19}{\rm m}^{-3}$; Figs.4(c) and (d) for $\overline{n_{\rm e}}$=1.5×10^{19}m^{-3} and Figs.4(e) and (f) for $\overline{n_{\rm e}}$=2×10^{19}m^{-3}. The profiles of the diffusion coefficient $D_k(r)$ are flat expect those for the CI and CII impurity particles, whose $D_k(r)$ values are low in the center of plasma. The diffusion coefficients $D_k(r)$ of impurities in other ionized states in a radial region of 1cm $< r <$25cm are about 1–1.9m^2/s for $\overline{n_{\rm e}}$=1×10^{19}m^{-3}; about 1–1.3m^2/s for $\overline{n_{\rm e}}$=1.5×10^{19}m^{-3} and about 0.85–1.2m^2/s for $\overline{n_{\rm e}}$=2×10^{19}m^{-3}. The diffusion coefficients $D_k(r)$ become low with the increase of electron density. In the plasma center region ($r <$10.8cm), the convection velocity $W_k(r)$ for $\overline{n_{\rm e}}$=1×10^{19}m^{-3} is positive and its maximum is 8.6m/s. In the center region ($r <$ 5.4cm), the convection velocity $W_k(r)$ at higher electron densities is also positive and its maxima are 0.42m/s for $\overline{n_{\rm e}}$=1.5×10^{19}m^{-3} and 0.22m/s for $\overline{n_{\rm e}}$ = 2×10^{19}m^{-3}. So the convections in these regions are outward and decrease with the electron density. In other radial regions up to about $r \sim$26 cm, the convections become inward and the absolute values of $W_k(r)$ decease with the electron density. In edge regions of $r >$ 26.3cm for $\overline{n_{\rm e}}$=1×10^{19}m^{-3} and $r >$ 26cm for $\overline{n_{\rm e}}$=1.5×10^{19}m^{-3}, the $W_k(r)$ values are positive and the convections outward. But the $W_k(r)$ values for $\overline{n_{\rm e}}$=2×10^{19}m^{-3} in these regions are negative and the convections inward. These results show clearly the reduced impurity transport at higher electron densities.

Figure 5 shows the total flux of the impurity ions Γ_k at different $\overline{n_{\rm e}}$. In the center plasma region (0 cm $\leq r \leq$ 20 cm), the contributions of the diffusion and the convection to the total flux of the impurity ions Γ_k are balanced, so the impurity particle fluxes are low. But in the edge plasma region ($r \geq$ 20 cm), the Γ_k increases rapidly with radius r and is outward. The diffusion makes the dominant contribution to the Γ_k. With the increase of $\overline{n_{\rm e}}$, the Γ_k decreases, which implies a reduction in transport.

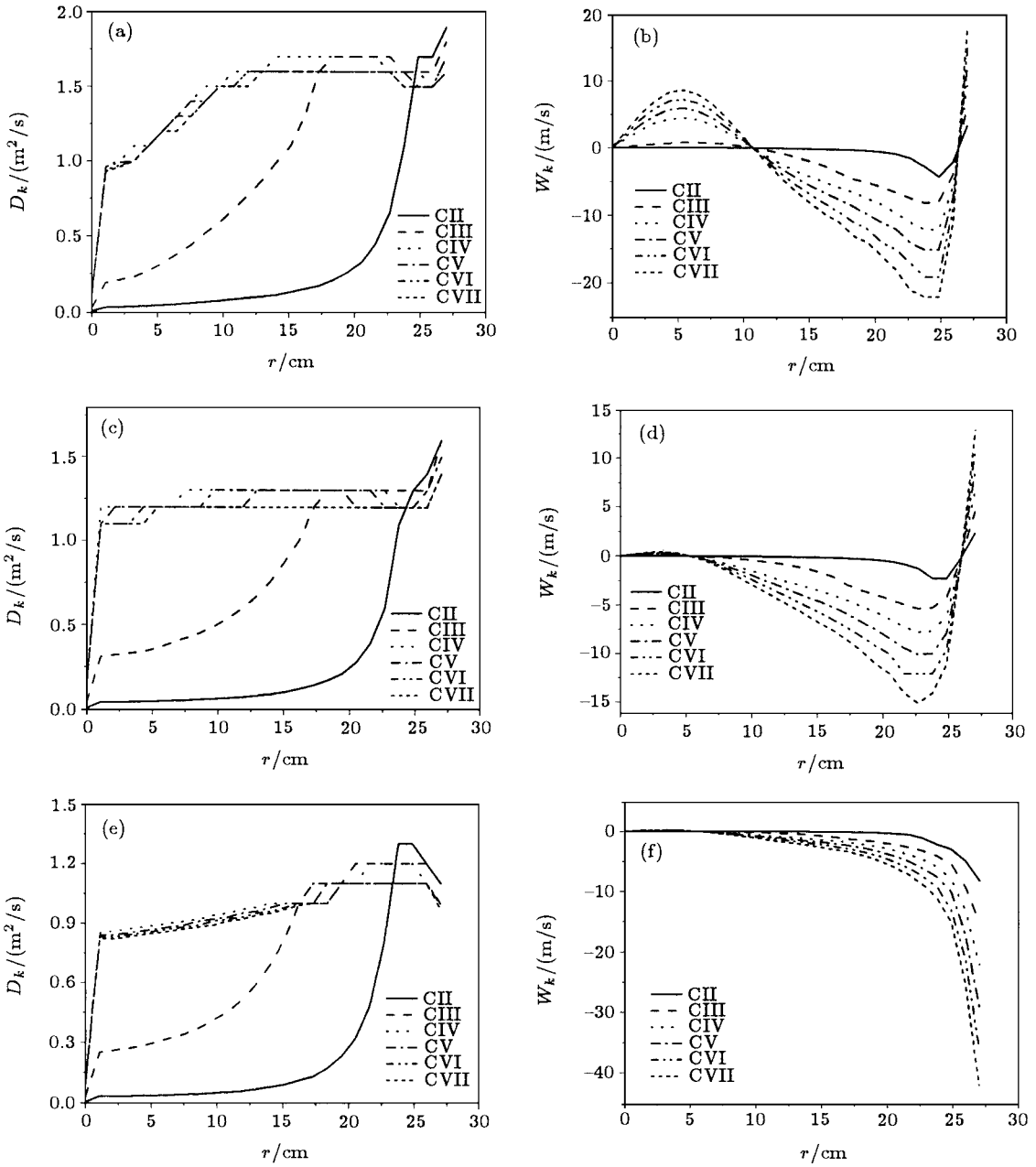


Fig.4. The diffusion coefficient $D_k(r)$ and the convection velocity $W_k(r)$ at different central line averaged electron densities $\overline{n_e}$. (a) and (b) show the $D_k(r)$ and $W_k(r)$, respectively, for $\overline{n_e}=1\times10^{19}m^{-3}$; (c) and (d) for $\overline{n_e}=1.5\times10^{19}m^{-3}$ and (e) and (f) for $\overline{n_e}=2\times10^{19}m^{-3}$.

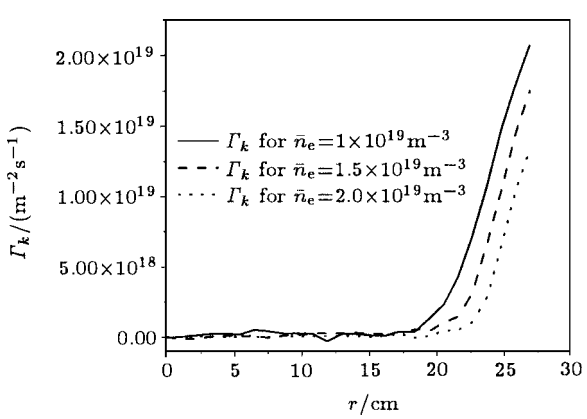


Fig.5. The simulation results of the total flux of the impurity ions Γ_k at different $\overline{n_e}$.

The confinement time of impurities τ_z can be defined as

$$\tau_z = \frac{N_z}{\Gamma_z(r_p)A|_{r_p}}, \tag{4}$$

where N_z is the total number of impurity ions of plasma, $\Gamma_z(r_p)$ is the outward impurity flux at the Last Closed Flux Surface (LCFS) and $A|_{rp}$ is the area of the LCFS. The N_z and $\Gamma_z(r_p)$ can be derived from the transport code. On the other hand, the global particle confinement time τ_p can be given by the H_α/D_α emission and electron density measurements. A comparison between τ_z and τ_p is made and shown in Fig.6.

It is clearly shown that τ_z and τ_p have the same trend with the increase of $\overline{n_e}$. The global particle and impurity particle transports reduce simultaneously with the increase of $\overline{n_e}$.

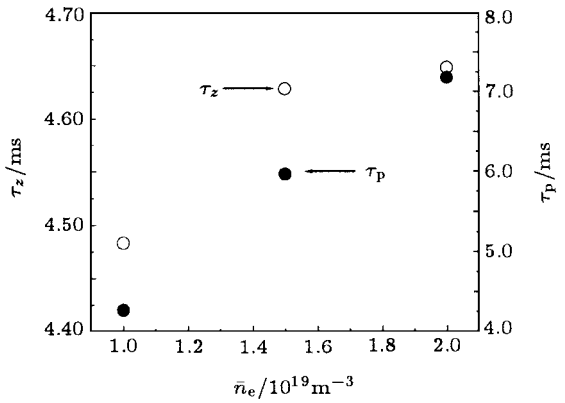


Fig.6. The global particle confinement time τ_p and the confinement time of impurity particles τ_z.

A comparison between measured results Z'_{eff} and simulation results Z_{eff} of the effective ionic charge of the plasma is made and shown in Fig.7. The measured results of Z'_{eff} are derived from visible bremsstrahlung measurements. The Z_{eff} decreases with the increase of $\overline{n_e}$, while Z'_{eff} also decreases. The simulation results Z_{eff} are about 3%–12.7% lower than the measured results Z'_{eff} because the contributions from oxygen and boron are not included. This result also clearly shows that the carbon is the dominant impurity in the HT-7 plasmas under the boronized wall condition.

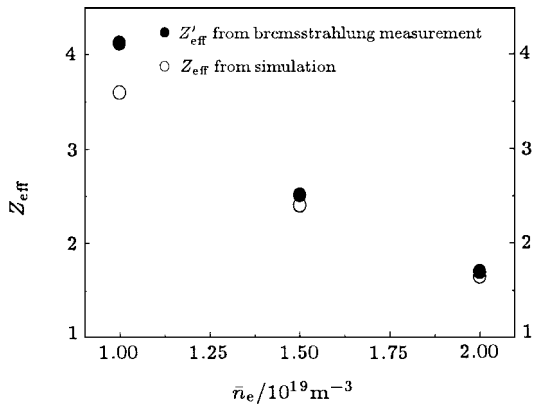


Fig.7. A comparison between measured and simulation results of Z_{eff} respectively against central line averaged electron densities $\overline{n_e}$.

The carbon ion densities of various ionized states $n_k(r)/n_0(r_p)$ at different $\overline{n_e}$ are obtained by simulation as shown in Fig.8. n_k(r) are normalized by $n_0(r_p)$, where $n_0(r_p)$ is the neutral carbon atom density at the edge of the plasma (r_p=27cm). With the increase of $\overline{n_e}$, the peak positions of the carbon ion densities of various ionized states move to the positions with slightly larger radii and the profiles of $n_0(r)$ show that the penetration depths of the neutral carbon atoms decrease.

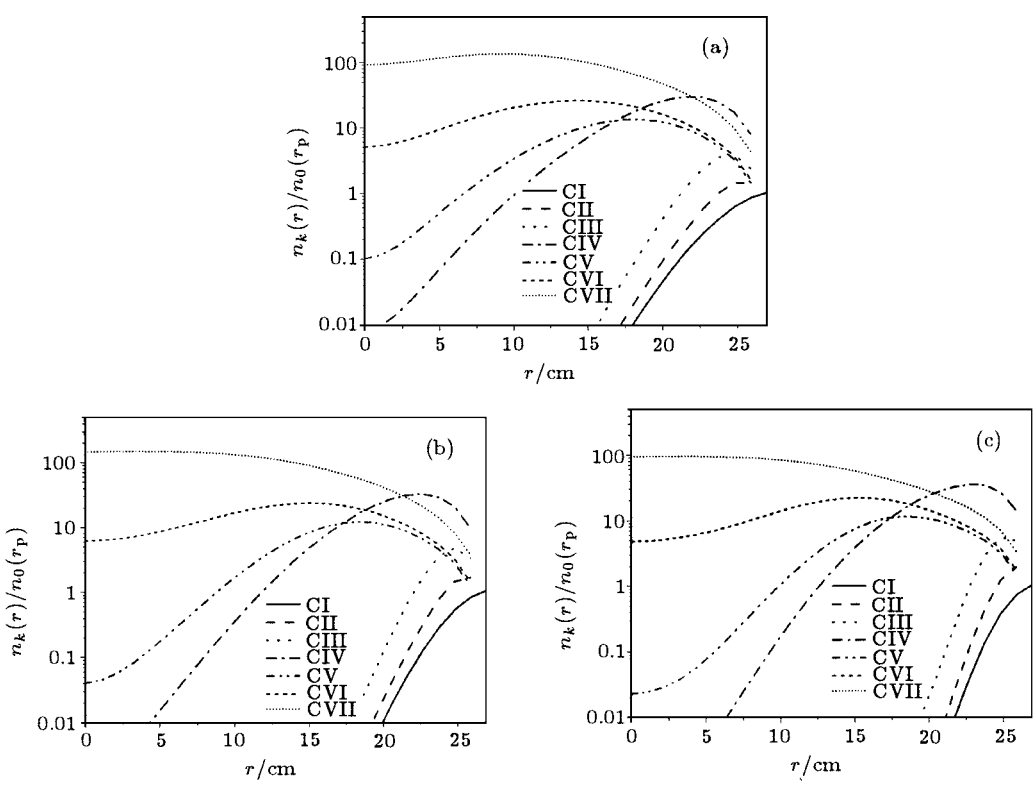


Fig.8. The simulation results of the impurity ion densities of various ionized states $n_k(r)/n_0(r_p)$ at different central line averaged electron densities $\overline{n_e}$: (a) $\overline{n_e} = 1 \times 10^{19}m^{-3}$; (b) $\overline{n_e} = 1.5 \times 10^{19}m^{-3}$; (c) $\overline{n_e} = 2 \times 10^{19}m^{-3}$.

6. Conclusion

The emissivity of CV at 227.1 nm is obtained by a special Abel inversion from the line-integrated optical measurements of impurity radiation profiles in the HT-7 tokamak.

An impurity transport code, which is based on the assumption that a cylindrical symmetry is present, is constructed. Both neoclassical and anomalous transports are taken into account in this code. The diffusion coefficient $D_k(r)$ and the convection velocity $W_k(r)$ are obtained by simulating the experimental results of the emissivity of line emission from ionized light impurities. This code also provides the impurity ion densities at various ionized states $n_k(r)/n_0(r_\mathrm{p})$.

The radial transport behaviours of carbon impurities at different central line averaged electron densities $\overline{n_\mathrm{e}}$ are investigated in the HT-7 tokamak. The results show clearly that the impurity transport decreases with the increase of $\overline{n_\mathrm{e}}$, correspondingly indicating the better confinement of impurity particles at higher $\overline{n_\mathrm{e}}$. The total flux of the impurity ions Γ_k increases rapidly with radius r in the edge region ($r \geq 20\,\mathrm{cm}$). The Γ_k decreases with the increase of $\overline{n_\mathrm{e}}$, which implies a reduction in impurity particle transport. Both τ_z and τ_p increase with the increase of $\overline{n_\mathrm{e}}$, correspondingly, the global particle and impurity particle transports reduce simultaneously. The effective ionic charges of the plasma Z_eff obtained from the measurements and the simulation have a similar relationship with the electron density. The simulation results are about 3%–12.7% lower than the experimental results, which implies that the carbon is the dominant impurity.

References

[1] Hawryluk R J and Suckewer S 1979 *Nucl. Fusion* **19** 607
[2] Hirshman S P and Sigmar D J 1981 *Nucl. Fusion* **21** 1079
[3] Song M, Wan B N *et al* 2003 *Plasma Phys. Control. Fusion* **45** 1805
[4] Stangeby P C *et al* 1990 *Nucl. Fusion* **30** 1225
[5] Stangeby P C 2000 *Plasma Phys. Control Fusion* **42** B271
[6] Beu T A *et al* 1985 *Comput. Phys. Commun.* **36** 161
[7] Wan B N, Zhao Y P, Li J G *et al* 2002 *Plasma Sci. Technol.* **4** 1375
[8] Wan B N and Yin F 1997 *Fusion Eng. Design* **34-35** 267
[9] Lotz W 1967 *IPP* **1** 62
[10] Goeler S von, Stodiek W, Eubank H, Fishman H, Grebenshchikov S and Hinnov E 1975 *Nucl. Fusion* **15** 301
[11] EUR-CEA, MAKOKOT—Code d'Evolution (August 1977)
[12] Hulse Russell A 1983 *Nuclear Technology/Fusion* **3** 259
[13] Ruan H L and Wan B N 2000 *International Journal of Infrared and Millimeter Waves* **21** 1973
[14] Ruan H L 2001 *Acta Phys. Sin.* **50** 2393 (in Chinese)
[15] Xu W 1997 PhD Thesis, Institute of Plasma Physics, Chinese Academy of Science, 55
[16] Jie Y X *et al* 2000 *Int. J. Infrared and Millimeter Waves* **21** 1375
[17] Shi Y *et al* 2002 *Nucl. Instr. Meth.* A **488** 566
[18] Liu S X 1997 *Acta Phys. Sin.* **46** 672 (in Chinese)
[19] Wan B N *et al* 1997 *Fusion Eng. Design* **34-35** 261